ORIGINAL ARTICLE

Journal of Cachexia, Sarcopenia and Muscle 2021; **12**: 1249–1265
Published online 1 July 2021 in Wiley Online Library (wileyonlinelibrary.com) **DOI:** 10.1002/jcsm.12749

Age-related decline in murine heart and skeletal muscle performance is attenuated by reduced Ahnak1 expression

Shokoufeh Mahmoodzadeh[1,2*], Katharina Koch[1], Cindy Schriever[1], Jingman Xu[1,3], Maria Steinecker[1], Joachim Leber[1], Elke Dworatzek[2,4], Bettina Purfürst[1], Severine Kunz[1], Deborah Recchia[5], Monica Canepari[5], Arnd Heuser[1], Silvia Di Francescantonio[1,6] & Ingo Morano[1]

[1]*Max-Delbrück-Center for Molecular Medicine in the Helmholtz Association (MDC), Berlin, Germany;* [2]*DZHK (German Centre for Cardiovascular Research), partner site Berlin, Berlin, Germany;* [3]*Heart Institute, School of Public Health, North China University of Science and Technology, Tangshan, China;* [4]*Charité-Universitaetsmedizin Berlin, Corporate Member of Freie Universitaet Berlin, and Berliner Institute of Health, Berlin, Germany;* [5]*Department of Molecular Medicine, University of Pavia, Pavia, Italy,* [6]*Experimental and Clinical Research Center, Charité-Universitaetsmedizin Berlin, Berlin, Germany*

Abstract

Background Aging is associated with a progressive reduction in cellular function leading to poor health and loss of physical performance. Mitochondrial dysfunction is one of the hallmarks of aging; hence, interventions targeting mitochondrial dysfunction have the potential to provide preventive and therapeutic benefits to elderly individuals. Meta-analyses of age-related gene expression profiles showed that the expression of Ahnak1, a protein regulating several signal-transduction pathways including metabolic homeostasis, is increased with age, which is associated with low VO_{2MAX} and poor muscle fitness. However, the role of Ahnak1 in the aging process remained unknown. Here, we investigated the age-related role of Ahnak1 in murine exercise capacity, mitochondrial function, and contractile function of cardiac and skeletal muscles.

Methods We employed 15- to 16-month-old female and male Ahnak1-knockout (Ahnak1-KO) and wild-type (WT) mice and performed morphometric, biochemical, and bioenergetics assays to evaluate the effects of Ahnak1 on exercise capacity and mitochondrial morphology and function in cardiomyocytes and tibialis anterior (TA) muscle. A human left ventricular (LV) cardiomyocyte cell line (AC16) was used to investigate the direct role of Ahnak1 in cardiomyocytes.

Results We found that the level of Ahnak1 protein is significantly up-regulated with age in the murine LV (1.9-fold) and TA (1.8-fold) tissues. The suppression of Ahnak1 was associated with improved exercise tolerance, as all aged adult Ahnak1-KO mice (100%) successfully completed the running programme, whereas approximately 31% male and 8% female WT mice could maintain the required running speed and distance. Transmission electron microscopic studies showed that LV and TA tissue specimens of aged adult Ahnak1-KO of both sexes have significantly more enlarged/elongated mitochondria and less small mitochondria compared with WT littermates ($P < 0.01$ and $P < 0.001$, respectively) at basal level. Further, we observed a shift in mitochondrial fission/fusion balance towards fusion in cardiomyocytes and TA muscle from aged adult Ahnak1-KO mice. The maximal and reserve respiratory capacities were significantly higher in cardiomyocytes from aged adult Ahnak1-KO mice compared with the WT counterparts ($P < 0.05$ and $P < 0.01$, respectively). Cardiomyocyte contractility and fatigue resistance of TA muscles were significantly increased in Ahnak1-KO mice of both sexes, compared with the WT groups. *In vitro* studies using AC16 cells have confirmed that the alteration of mitochondrial function is indeed a direct effect of Ahnak1. Finally, we presented Ahnak1 as a novel cardiac mitochondrial membrane-associated protein.

Conclusions Our data suggest that Ahnak1 is involved in age-related cardiac and skeletal muscle dysfunction and could therefore serve as a promising therapeutical target.

Keywords Ahnak1; Age-related mitochondrial dysfunction; Physical performance; Heart; Skeletal muscle

Received: 8 January 2021; Revised: 13 May 2021; Accepted: 8 June 2021
**Correspondence to: Shokoufeh Mahmoodzadeh, Max-Delbrück-Center for Molecular Medicine in the Helmholtz Association (MDC), Robert-Roessle-Str. 10, 13125 Berlin, Germany. Phone: +49 30 9406 3483, Fax: +49 30 9406 227, Email: shokoufeh.mahmoodzadeh@mdc-berlin.de*

Introduction

United Nations' estimates predict that every sixth individual worldwide will be aged 65 years or over by 2050.[1] Increasing life expectancy *per se* is a positive human development. However, aging is associated with several undesirable aspects and predisposes the elderly to age-related diseases such as cardiovascular diseases, cancer, neurodegenerative diseases, and metabolic disorders, which are major causes of disability worldwide.[2] Among these, cardiovascular diseases account for approximately 40% of age-related diseases and their prevalence increases drastically with age.[3] One of the most important physiological changes that occur with aging is a decline in cardiorespiratory fitness leading to physical inactivity, contributing to skeletal muscle atrophy and dysfunction.[4,5] On the other hand, as a normal part of the aging process, older individuals lose skeletal muscle mass, strength, and function, known as sarcopenia.[6] The progressive loss of muscle mass and strength in the elderly plays a significant role in limiting exercise capacity that in turn increases the risk of cardiovascular morbidity and mortality.[5,7] Therefore, we are in critical need of a detailed mechanistic understanding of the pathogenesis of cardiac and skeletal muscle aging and the identification of therapeutic targets to slow down the age-related decline in cardiovascular and skeletal muscle functions.

Although the exact biological and cellular mechanisms responsible for the aging of the heart and skeletal muscle are not known, new evidence increasingly indicates that mitochondrial dysfunction is heavily implicated in this process.[8,9] Both muscles are tissues with high-energy demand and thus high mitochondrial density. Indeed, aged heart and skeletal muscle display multiple abnormalities in mitochondrial morphology, biogenesis, dynamics, quality control, respiratory function, susceptibility of the mitochondrial permeability transition pore, and reactive oxygen species production.[8] To date, therapies or drug-based approaches to restore mitochondrial function in aged striated muscular tissues do not exist. Therefore, interventions improving mitochondrial function are attractive targets to attenuate cardiac and skeletal muscle dysfunction and to extend health span in the elderly.

Ahnak1 (also known as desmoyokin), a protein of an exceptionally large size (≈700 kDa), is localized mainly on the plasma membrane in striated muscle types.[10] Ahnak1 has been implicated in diverse signal transduction processes affecting cell differentiation and proliferation; organization of the plasma membrane architecture; and regulation of extracellular Ca^{2+} influx, vascular healing, tumour metastasis, DNA-repair, and adipogenesis.[11] Several studies have shown a positive correlation between Ahnak1 gene expression and age.[12–14] Interestingly, increased expression of Ahnak1 was associated with low VO_{2MAX} and poor muscle fitness.[15] However, the exact biological function of Ahnak1 in the aging process of the heart and skeletal muscle is unknown.

To understand the link between Ahnak1 expression and muscle fitness at advanced age, we subjected aged adult Ahnak1 knockout mice (Ahnak1-KO) and their age-matched wild-type (WT) siblings of both sexes to 4 weeks of treadmill running. Aged adult Ahnak1-KO mice exhibited enhanced running performance compared with their WT counterparts, suggesting that attenuated Ahnak1 expression in aged adult mice might improve mitochondrial function at basal level. Indeed, our data clearly demonstrate that suppression of Ahnak1 significantly ameliorates age-related mitochondrial dysfunction, resulting in improved cardiomyocyte contractility and increased resistance to anterior tibialis (TA) muscle fatigue in aged adult mice. These data suggest that the suppression of Ahnak1 expression may improve overall physical fitness and prevent adverse health outcomes with advancing age.

Material and methods

Animals

Fifteen- to 16-month-old male and female homozygous Ahnak1-KO[10] and their WT littermates were used. The animals were kept on a 12:12 h light–dark cycle in temperature-controlled rooms and fed with commercial standard chow and water ad libitum. All animal experiments were approved by and conducted in accordance with the guidelines set out by the State Agency for Health and Social Affairs (LaGeSo, Berlin, Germany) and with the ethical standards laid down in the 1964 Declaration of Helsinki and its later amendments.

Treadmill running

Aged adult female and male mice of both genotypes were assigned to treadmill running or sedentary control (n = 10–16). Over a 2 week period, mice were acclimated to the treadmill via a gradual increase of the training intensity (10–20 cm/s, at a 5° incline, 10–60 min/day/mouse). After the adaptation phase, mice were trained with a maximal training capacity {12–20 cm/s [2 min (12 cm/s); 2 min

(14 cm/s); 2 min (16 cm/s); 4 min (18 cm/s); 50 min (20 cm/s)] at a 5° incline} over a period of 4 weeks for 60 min/day/mouse and 5 days/week. Exclusion criterion was defined as the mouse's inability to continue regular treadmill running and to maintain the required running speed and distance despite mechanical prodding.

Analysis of body composition

Whole body composition of live animals (body weight, fat, and muscle mass) was determined using the time-domain-nuclear-magnetic-resonance imaging (Bruker MiniSpec LF90II).

Cell culture and treatment

Ventricular mouse cardiomyocytes were isolated by a standard enzymatic technique as described before.[16] Briefly, after cervical dislocation, hearts were rapidly removed and perfused at 37°C for 10 min with a bicarbonate buffer (pH 7.4) containing low Ca^{2+} and collagenase (type II; PAN BIOTECH). Subsequently, the ventricles were minced, and isolated cardiomyocytes were resuspended in M199 medium (Sigma) supplemented with 0.2% BSA, 10% foetal calf serum, 5 mmol/L creatine, 5 mmol/L taurine, 2 mmol/L carnitine, 10 μmol/L cytosine-D-arabinofuranoside, and antibiotics. Cardiomyocytes were seeded in with 0.2% laminin-coated well-plates and incubated in a 5% CO_2 incubator at 37°C to allow myocyte attachment. After 2 h, media were replaced with appropriate media for further functional analysis (as described further).

For *in vitro* investigations, we used a human adult left ventricular cardiomyocyte cell line, the AC16 cells,[17] which were cultured as previously described.[18] To achieve a transient knock-down of Ahnak1 in AC16 cells, a set of three different Stealth siRNAs (small interfering RNA) against human Ahnak1 (HSS149070, HSS149071, HSS149072, ThermoFisher Scientific) were transfected into AC16 cells using Lipofectamine RNAiMAX transfection reagent (Invitrogen Life Technologies) according to the manufacturer's instructions. The Stealth siRNA negative control (12935112, ThermoFisher Scientific) was used to evaluate the siRNA specificity (scramble-siRNA). Mock-transfected cells (treated with transfection reagent only) were employed to verify any non-specific effects caused by the transfection reagent or process. For further details, see the Supporting Information, *Data* S1.

Gene expression analysis

Total RNA extraction and quantitative real-time polymerase chain reaction were conducted as previously described.[19] Briefly, total RNA was isolated from mouse hearts, TA muscles, or AC16 cells by using TRIzol reagent (Invitrogen, UK) according to the manufacturer's instructions. Quantitative real-time polymerase chain reaction experiments were performed using a StepOnePlus Real-Time PCR System (Applied Biosystems) with Power SYBR Green PCR Master Mix (Applied Biosystems) and gene-specific primers. Primer sequences are listed in the Supporting Information, *Table* S1. Hypoxanthine phosphoribosyltransferase (*Hprt*) and/or glyceraldehyde 3-phosphate dehydrogenase (*Gapdh*) were used as endogenous references, as indicated, to normalize expression of the target genes.

Western blot analysis

Whole protein lysates isolated from left ventricle (LV) and TA muscle tissues from WT and Ahnak1-KO mice of both sexes, and AC16 cells were separated by SDS-polyacrylamide gel electrophoresis and electrotransfered to Nylon membrane as described before.[20,21] Antibodies used are listed in the Supporting Information, *Table S2*. The signal was visualized with the ECL™ detection kit (GE Healthcare). Band intensities were quantified with Image Lab software 5.1 V (Bio-Rad Laboratories).

Cardiomyocyte contractile assessment

Contractile properties of cardiomyocytes isolated from female and male aged adult Ahnak1-KO and WT-littermate hearts (n = 5–6 mice per group) were measured using a video-based edge detection system (IonOptix Limited, Dublin, Ireland) as described before.[18] Briefly, freshly isolated attached cardiomyocytes (2×10^4 cells per well) cultured on laminin-coated coverslips were washed twice with Hank's balanced salt modified buffer (pH 7.4) for 15 min at 37°C and electrically field-stimulated with bipolar pulses of 5 ms duration at 1 Hz. Cell shortening and relaxation of arbitrarily selected stimulated cardiomyocytes were recorded using IonWizard Transient Analysis software package (IonOptix Limited) together with an Olympus IX70 inverted microscope (40× objective) (Myocyte Calcium & Contractility Recording System; IonOptix Limited).

Oxygen consumption rate

The oxygen consumption rate (OCR) was measured using Seahorse XFe96 analyser (Agilent Technologies) and carried out in accordance with the procedures described in the Seahorse XF Cell Mito Stress Test kit (Agilent Technologies). Measurements were performed in freshly isolated cardiomyocytes (5×10^3 cells per well) from aged adult female and male Ahnak1-KO and WT hearts as well as in AC16 cells (8×10^3 cells per well) transfected with

DOI: 10.1002/jcsm.12749

Ahnak1-siRNA, neg-siRNA or mock-transfected. For further details on OCR measurement, please see the Supporting Information, *Data* S1. Upon completion of the assays, data were normalized for protein content of cells. OCR profiles were expressed as pmol O_2/min/μg protein. All parameters [rates of basal respiration, max. respiration, spare (reserve) respiratory capacity (the difference between the max. respiration and the basal mitochondrial respiration), and ATP production] were calculated using Wave Software according to manufacturer (Agilent Technologies). Twelve replicates were run for each condition, and experiments were repeated seven times independently.

Mitochondrial isolation for electron microscopy and for mitochondrial subfractionation analysis

Mitochondria and fractions of mitochondrial matrix and mitochondrial membrane were isolated from freshly excised hearts of aged adult Ahnak1-KO and WT littermates of both sexes (n = 3–4) with Mitochondria Isolation Kit for Tissue (Thermo Scientific™) according to manufacturer's instruction (for further details, please see the Supporting Information, *Data* S1).

Transmission electron microscopy, sample preparation, and imaging

For morphological analysis, TA tissues from aged adult female and male Ahnak1-KO and WT mice (n = 4 per group) were dissected and fixed by immersion with 2% (w/v) formaldehyde/2.5% (v/v) glutaraldehyde in 0.1 M phosphate buffer for 24–48 h. Whole murine heart from aged adult Ahnak1-KO and WT mice of both sexes (n = 6 per group) were dissected and externally perfused with 4% (w/v) formaldehyde/0.5% (v/v) glutaraldehyde in 0.1 M phosphate buffer. Tissue from the LV was further dissected and fixed with 2.5% (v/v) glutaraldehyde in 0.1 M phosphate buffer for 24–48 h. After switching to 0.1 M cacodylate buffer, tissue blocks were post-fixed with 1% (v/v) osmium tetroxide, dehydrated in a graded series of ethanol, and embedded in the PolyBed® 812 resin (Polysciences Europe GmbH). Ultrathin sections (60–80 nm) were stained with uranyl acetate and lead citrate before image acquisition.

For immunolabelling, isolated mitochondria were fixed with 4% (w/v) formaldehyde for 1 h at room temperature (RT). Samples were further processed as described by Slot and Geuze.[22] Briefly, samples were solidified in 12% (w/v) gelatine, infiltrated with 2.3 M sucrose, frozen in liquid nitrogen, and sectioned (Ultracut E, Leica microsystems) at cryo temperatures. Sections were blocked and washed in phosphate-buffered saline supplemented with 5% BSA/0.1% fish skin gelatine/5% goat serum/0.1% glycine for 30 min at RT. Labelling was performed with a primary anti-Ahnak1 antibody (E-5, Santa Cruz) for 1 h at 4°C and a secondary anti-mouse 12 nm colloidal gold conjugate (115-205-146, Dianova) for 30 min at RT. Sections were contrasted with 3% tungstosilicic acid hydrate (w/v) in 2.8% polyvinyl alcohol (w/v).[23]

All samples were examined with a Morgagni electron microscope (Thermo Fisher). Acquisition was performed with a Morada CCD camera and the iTEM software (Emsis GmbH, Germany). For analyses of mitochondrial size (surface area), 10 micrographs were taken for each LV and TA tissue to measure mitochondrial size per unit area (48 μm^2) in a blinded fashion.

There are two different pools of mitochondria within the cardiomyocytes and TA muscles, namely, the subsarcolemmal mitochondria and the intermyofibrillar mitochondria. In this study, we focused on the analysis of the intermyofibrillar mitochondria population because several studies have reported that this population of mitochondria is more susceptible to aging than subsarcolemmal mitochondria.[24–27]

Ex vivo contraction of isolated tibialis anterior muscle

The method used for mechanical analysis of intact muscles was described previously.[28] TA muscle from aged adult male Ahnak1-KO (n = 16), male WT (n = 10), female Ahnak1-KO (n = 11), and female WT (n = 7) mice was dissected, transferred to an organ bath containing Krebs solution (vol. 20 mL) bubbled with 95% O_2 and 5% CO_2 and kept at constant temperature (22°C) where it was mounted between the hook of a force transducer (FT-03; AstroNova) and a hook connected to a movable shaft that was used to adjust the muscle length. The muscle was tied to the hooks by means of silk threads that had been previously fixed to the tendons. On both sides of the perfusion bath at distance of about 2 mm from the preparation, plate platinum electrodes connected with a stimulator (S48 Grass-stimulator; AstroNova) allowed electrical field stimulation. The muscle was stretched to Lo (muscle optimal length), and its response to electrical stimulation was tested. Tetanic isometric contractions were evoked (110 Hz, 120 ms, supramaximal amplitude) at Lo. A fatigue test was performed by measuring the drop-in force of the maximal tetanic force following 20 repeated contractions in a ramp protocol at 0.03, 0.09, and 0.3 Hz. A 1401 A/D converter (Cambridge Electronic Design) and CEA Spike2 software (Cambridge Electronic Design) were used for the analysis. The muscle isolated from its motor neuron and stimulated using a constant electrical field allows to distinguish the neural fatigue from the intrinsic muscle fatigue due to metabolic properties of the muscle.

Statistics

All data are presented as mean ± standard error of the means. Statistical analysis was performed using one-way analysis of variance followed by Bonferroni *post hoc* test to compare multiple groups, two-way analysis of variance followed by Bonferroni *post hoc* test to compare means, two-tailed Student's *t*-test to compare values between two groups, or multiple *t*-test, as appropriate, using GraphPad Prism 5.01. A value of $P < 0.05$ was considered statistically significant.

Results

Aged adult Ahnak1-KO mice show improved exercise tolerance

Aging-specific array-based gene expression analyses in skeletal muscles showed that increased Ahnak1 expression was positively associated with aging.[13–15] In agreement, we also showed that the expression of Ahnak1 protein was significantly higher (≈1.9-fold) in the LV tissue of aged adult Ahnak1-WT mice (16 months old) compared with young Ahnak1-WT mice (2 months old; *Figure* 1A).

Because previous studies showed that increased Ahnak1 expression is associated with a low VO_{2MAX} and poor skeletal muscle fitness,[14,15] we determined whether the lack of Ahnak1 affects the physical fitness in aged adult mice. Surprisingly, all aged adult Ahnak1-KO mice (100%) successfully completed the treadmill running programme (*Figure* 1B). While all Ahnak1-KO mice kept running at higher speed for 4 weeks, most age and sex-matched WT mice were not able to run consistently from the beginning of the training programme. In total, only 8% of the female and 31% of the male WT mice were able to complete the running programme (*Figure* 1B). These data showed that Ahnak1-KO mice have a distinctly improved exercise capacity.

The body composition analysis revealed no significant changes in body weight, fat, and muscle mass between aged adult female and male Ahnak1-KO and their age-matched WT

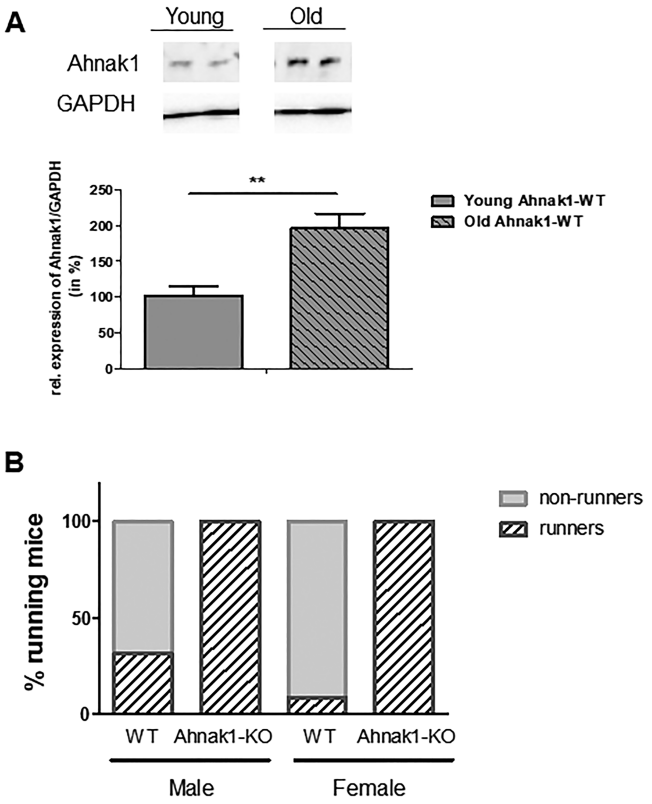

Figure 1 Increased Ahnak1 expression is associated with reduced running capacity in old WT mice. (A) The level of Ahnak1 protein is increased in murine heart with aging. Upper panel: Representative immunoblots for Ahnak1 and GAPDH (20 μg lysate/lane) in the left ventricular tissues of young and aged adult Ahnak1-WT littermates ($n = 7$ hearts per group). Lower panel: expression of Ahnak1 as the relative band intensity to GAPDH band intensity ratio (in %). $^{**}P < 0.05$, Student's unpaired *t*-test. (B) Treadmill exercise test. After acclimatization, exercise training was performed on a treadmill over a period of 4 weeks for 1 h/day and 5 days/week. The graph represents the percentage of mice that were able to complete the running programme over 4 weeks (runners) and which were not able to run from the beginning (non-runners). $n = 10–16$ mice per group. WT, wild type.

DOI: 10.1002/jcsm.12749

mice (Supporting Information, *Figure* S1A). Additionally, we observed no significant changes in the heart or TA wet masses between both genotypes (Supporting Information, *Figure* S1B). Therefore, we can rule out the contribution of these factors to the observed differences in our model.

Ahnak1 is involved in the regulation of mitochondrial size and mitochondrial activity in the heart

Because aged adult Ahnak1-KO mice revealed a superior physical fitness, we hypothesized that the mitochondria of aged adult Ahnak1-KO mice show overall improved function. To test this hypothesis, we compared mitochondrial morphology and activity in the hearts of male and female aged adult Ahnak1-KO and WT-littermate mice at basal level. On average, the size of cardiac mitochondria is between 0.5 and 1 μm^2.[29] Quantitative analysis of mitochondrial size in electron micrographs showed that cardiomyocytes of aged adult Ahnak1-KO mice of both sexes oppose significantly less small (<0.5 μm^2) and more large (>1 μm^2) mitochondria compared with sex-matched WT mice (*Figure* 2A, 2B and 2D). There were no significant differences in the number of medium-sized mitochondria ($0.5 < X < 1$ μm^2) between both genotypes (*Figure* 2C).

Because mitochondria are capable of modulating their size and shape by fusion or fission processes,[30] we assessed the effect of Ahnak1 on the expression of genes involved in mitochondrial fusion and fission in the LV tissues of aged adult WT and Ahnak1-KO mice of both sexes. Key markers of mitochondrial fusion include mitofusin 1 and 2 (*Mfn1* and *Mfn2*) and optic atrophy 1 (*Opa1*). Mitochondrial fission is mainly mediated by dynamin-related protein 1 (*Drp1*) and mitochondrial fission 1 protein (*Fis1*). In accordance with previous studies,[30,31] we observed no significant differences in the expression of representative marker genes involved in the fusion and fission processes in the hearts of aged adult WT and Ahnak1-KO mice (Supporting Information, *Figure* S2).

Further, we investigated whether changes in mitochondrial size contribute to improved mitochondrial activity in cardiomyocytes of aged adult Ahnak1-KO mice. Evaluation of OCR showed that both maximal respiratory activity and the respiratory reserve capacity (spare capacity) were significantly higher in cardiomyocytes prepared from aged adult Ahnak1-KO hearts compared with WT mice (*Figure* 2E–2G). These data indicate that overall mitochondrial activity in aged adult Ahnak1-KO cardiomyocytes is improved, and Ahnak1 might be a key modulator of bioenergetics capacity of cardiomyocytes in old mice.

Mitochondrial content in the heart lysates from aged adult male and female WT and Ahnak1-KO mice was determined by quantifying the expression of representative subunits of key proteins involved in mitochondrial oxidative phosphorylation (complexes I, II, III, IV, and the ATP synthase, OXPHOS system). As shown in *Figure* 2H, only the protein level of representative subunits of complexes III (UQCRC2) and V (ATP5a) was significantly increased in the hearts of aged adult Ahnak1-KO mice, when compared with WT littermates.

Collectively, these results suggest that the suppression of Ahnak1 in aged adult mouse hearts is sufficient to alter the mitochondrial morphology and to improve the oxidative capacity of cardiomyocytes.

Deletion of Ahnak1 is associated with significantly improved contractile function in cardiomyocytes of the aged adult heart

To assess whether the effect of improved mitochondrial activity in aged adult Ahnak1-KO cardiomyocytes can be extrapolated to a better contractile function of cardiomyocytes, the contractile parameters were compared between cardiomyocytes from aged adult female and male Ahnak1-KO and WT hearts. Our data demonstrated that, in comparison with cardiomyocytes from aged adult WT hearts, cardiomyocytes from both sexes of Ahnak1-KO mice exhibited a significant increase in shortening amplitude (*Figure* 3A) and in the maximal rate of contraction and relaxation velocities ($-$dL/dt and +dL/dt, *Figure* 3B–3C), resulting in a lower time to peak shortening (*Figure* 3D) and shorter relaxation times (*Figure* 3E) as measured at 50% of shortening and relengthening, respectively. These data suggest that the remodelled mitochondria in aged adult Ahnak1-KO cardiomyocytes are associated with significantly improved contractile function, supporting these as a more primary effect of Ahnak1 absence.

Ahnak1 regulates mitochondrial morphology and function in tibialis anterior muscle

In this study, we used TA muscles because it has been shown that their mitochondrial function decline with aging.[32] As previously reported,[13–15] we also showed that the expression of Ahnak1 protein was significantly higher (≈1.8-fold) in the TA tissues of aged adult Ahnak1-WT mice (16 months old) compared with young Ahnak1-WT mice (3 months old; *Figure* 4A). To assess whether Ahnak1 deficiency is also associated with an alteration of the mitochondrial morphology in skeletal muscles, longitudinal sections of TA muscle tissues of aged adult WT and Ahnak1-KO mice of both sexes ($n = 4$ per group) were analysed. *Figure* 4B (left) shows a representative transmission electron microscopy-micrograph from the central part of a typical WT TA-muscle fibre with regularly arranged sarcomeres. Most mitochondria are small and situated at

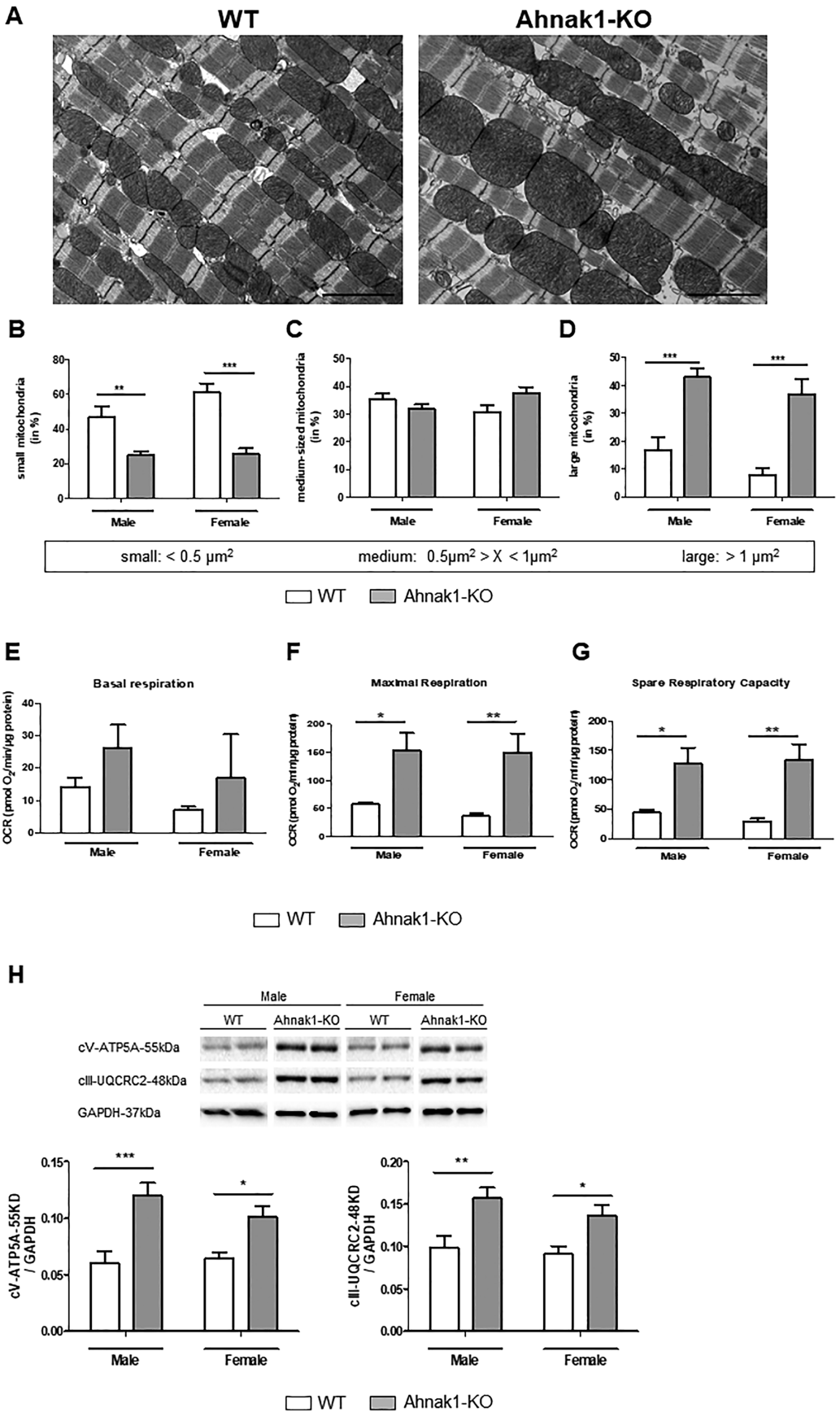

DOI: 10.1002/jcsm.12749

Figure 2 Ahnak1 directly modulates mitochondrial size and activity in aged mouse hearts. (A–D) Mitochondrial size is increased in aged Ahnak1-KO hearts. (A) Representative electron micrographs of left ventricular sections from 15–16 months old WT (left) and Ahnak1-KO (right) mice. 11 000× magnification; scale bar: 2 μm. (B–D) The graphs represent the percentage of the number of small-sized (B), medium-sized (C), and large-sized (D) mitochondria per image area (48 μm^2) in the left ventricular sections from aged adult female and male WT and Ahnak1-KO mice. *n* = 6 mice/group. (E–H) Mitochondrial activity is improved in aged Ahnak1-KO hearts. (E–G) parameters of respiratory control in the cardiomyocytes isolated from aged adult female and male Ahnak1-KO hearts. (E) Basal respiration. (F) Mitochondrial max. respiration. (G) Reserve (spare) respiratory capacity. OCR, oxygen consumption rate. *n* = 7 hearts/group. (H) Representative western blot (upper panel) and quantification analysis (lower panel) of the level of complexes III (UQCRC2) and V (ATP5a) subunits of OXPHOS in heart lysates of aged adult WT and Ahnak1-KO mice of both sexes; the loading control was GAPDH. *n* = 7–8 hearts/group. All data are expressed as means ± SEM. $^*P < 0.05$, $^{**}P < 0.01$, $^{***}P < 0.001$, two-way analysis of variance followed by Bonferroni *post hoc* test. WT, wild type.

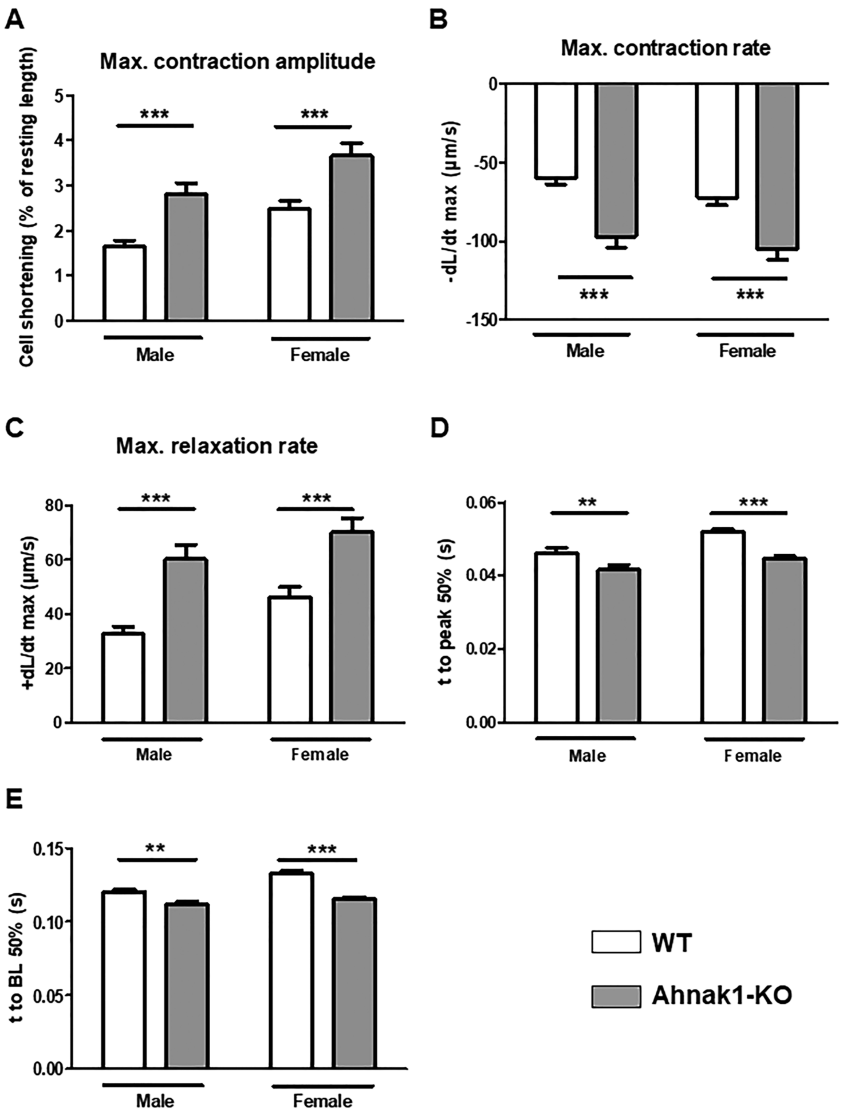

Figure 3 Ahnak1 deficiency is associated with improved contractile function of aged adult cardiomyocytes. Contractile parameters from isolated primary cardiomyocytes of aged adult female and male Ahnak1-KO and WT littermates were quantified by (A) max. contraction shortening, (B) maximal rate of contraction (−dL/dt) and (C) maximal rate of relaxation (+dL/dt) velocities; (D) time to 50% contraction (peak), and (E) time to 50% re-lengthening (BL, base line). *n* = 48–51 cardiomyocytes from five to six hearts per group. All data are expressed as means ± SEM. $^{**}P < 0.01$, $^{***}P < 0.001$, two-way analysis of variance followed by Bonferroni *post hoc* test. WT, wild type.

both sides of Z lines (arrows). *Figure* 4B (right) displays a representative transmission electron microscopy-micrograph from the central part of a typical Ahnak1-KO TA muscle fibre. In addition to the small mitochondria located on both sides of the Z lines (arrows), the image shows a series of enlarged/elongated mitochondria (asterisks) separated by regularly

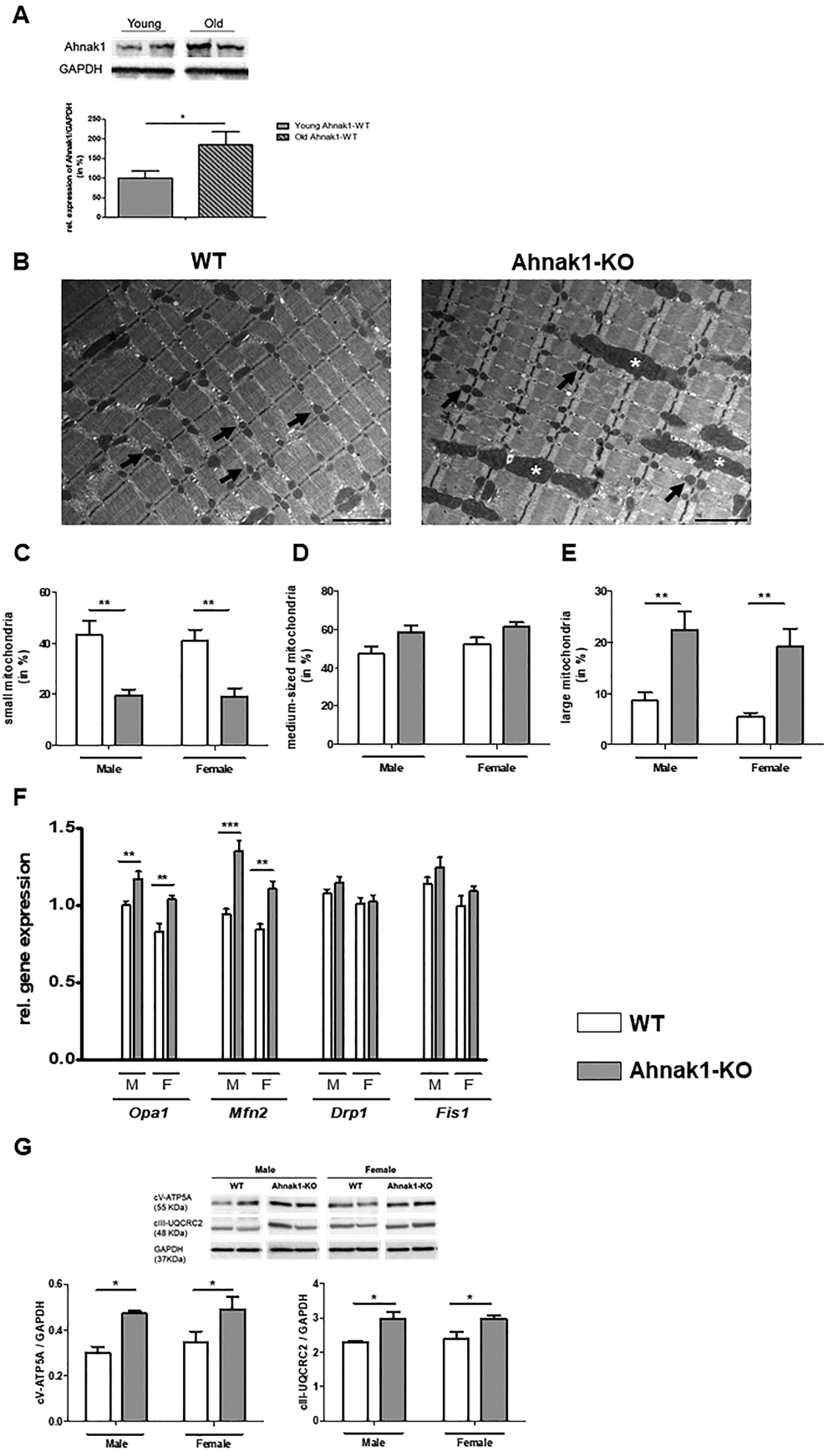

DOI: 10.1002/jcsm.12749

Figure 4 Deletion of Ahnak1 is associated with significantly increased mitochondrial function in aged adult tibialis anterior (TA) muscles. (A) The level of Ahnak1 protein is increased in murine TA muscle with aging. Upper panel: representative immunoblots for Ahnak1 and GAPDH (20 μg lysate/lane) in the TA muscle tissues of young and aged adult Ahnak1-WT littermates (n = 7 hearts/group). Lower panel: expression of Ahnak1 as the relative band intensity to GAPDH band intensity ratio (in %). *$P < 0.05$, Student's unpaired t-test. (B) Representative electron micrographs of longitudinal sections of TA muscle fibres of aged adult WT (left) and Ahnak1-KO mice (right). Small mitochondria (arrows), enlarged/elongated mitochondria (asterisks). 8100× magnification; scale bar: 2 μm. (C–E) The percentage of the number of small-sized (C), medium-sized (D), and large-sized (E) mitochondria per image area (48 μm^2) in TEM-micrographs acquired from TA tissues. n = 4 mice/group. (F) Expression levels of fusion and fission markers in TA muscles of aged adult WT and Ahnak1-KO mice. Expression of target genes was normalized to the geometric mean of *Hprt* and *Gapdh*. n = 6–8 mice per group. (G) Representative western blots (upper panel) and quantification analysis (lower panel) of the level of complexes III (UQCRC2) and V (ATP5a) subunits of OXPHOS in TA muscle lysates of aged adult WT and Ahnak1-KO mice; the loading control was GAPDH. n = 4 mice/group. All data are expressed as means ± SEM. *$P < 0.05$, **$P < 0.01$, ***$P < 0.001$, two-way ANOVA followed by Bonferroni *post hoc* test. WT, wild type.

arranged sarcomeres. Quantitative analysis of mitochondrial size showed that the TA muscles of aged adult Ahnak1-KO mice display significantly less small (<0.05 μm^2) and more large/elongated (>0.2 μm^2) mitochondria compared with those of sex-matched WT mice (*Figure* 4C and 4E). There were no significant differences in the number of medium-sized mitochondria ($0.05 < X < 0.2$ μm^2) between both genotypes (*Figure* 4D). Taken together, our results demonstrate that mitochondrial morphology is also changed in the TA muscles of aged adult Ahnak1-KO mice.

Next, we assessed the effects of Ahnak1 deficiency on expression of genes involved in mitochondrial fusion and fission in TA muscle tissues of aged adult male and female WT and Ahnak1-KO mice. As shown in *Figure* 4F, aged adult Ahnak1-KO mice showed a significantly higher expression of mitochondrial fusion markers, *Opa1* and *Mfn2*, in their TA muscle tissues compared with those of WT mice, while the expression of mitochondrial fission markers *Fis1* and *Drp1* was unchanged, which could be a possible explanation for the presence of more large and elongated mitochondria in the TA muscles of Ahnak1-KO mice.

Further analysis of TA muscle tissues revealed that only protein levels of the representative subunits of complexes III (UQCRC2) and V (ATP5a) were significantly increased in TA muscles of aged adult Ahnak1-KO mice, when compared with those from WT littermates (*Figure* 4G).

These results are evidence that, as in cardiomyocytes, Ahnak1 is also involved in the regulation of mitochondrial morphology and function in the TA muscle of aged adult mice.

Deletion of Ahnak1 is associated with significantly increased fatigue resistance in aged adult tibialis anterior muscle

To assess whether the remodelled mitochondria in aged adult Ahnak1-KO TA muscle can contribute to improved skeletal muscle fitness and exercise capability, the response to fatigue of TA muscles from aged adult Ahnak1-KO and WT mice was examined. Results showed that the TA muscles from aged adult Ahnak1-KO mice of both sexes are significantly more fatigue resistant than those of age-matched WT mice (*Figure* 5). These data suggest that the remodelled mitochondria in aged adult Ahnak1-KO TA muscles are associated with significantly improved contractile function in TA muscles confirming them as a target of Ahnak1.

Down-regulation of Ahnak1 improves mitochondrial function in a human left ventricular cardiomyocyte cell line

To determine whether Ahnak1 is directly involved in the regulation of mitochondrial function, AC16 cells (6×10^3 cells per well) were transfected with specific Ahnak1-targeted siRNA

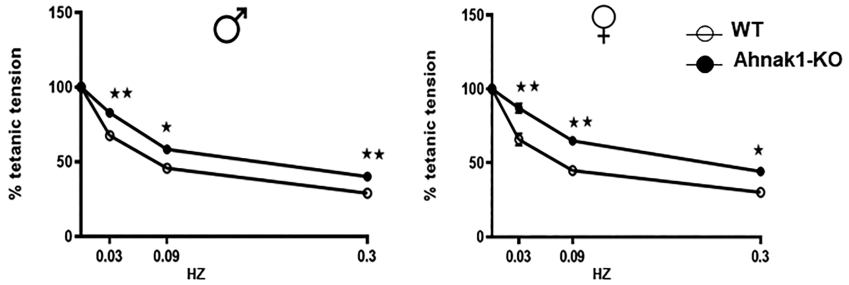

Figure 5 Ahnak1 deficiency is associated with significantly enhanced fatigue resistance in aged adult tibialis anterior (TA) muscle. Fatigue index in isolated TA muscles from aged adult male Ahnak1-KO (n = 16) and WT (n = 10) mice (left panel), and female Ahnak1-KO (n = 11) and WT (n = 7) mice (right panel) expressed as a percentage of the maximal tetanic force. TA muscles were subjected to 20 repeated contractions in a ramp protocol at 0.03, 0.09, and 0.3 Hz. The data are expressed as means ± SEM, *$P < 0.05$; **$P < 0.001$, multiple t-test.

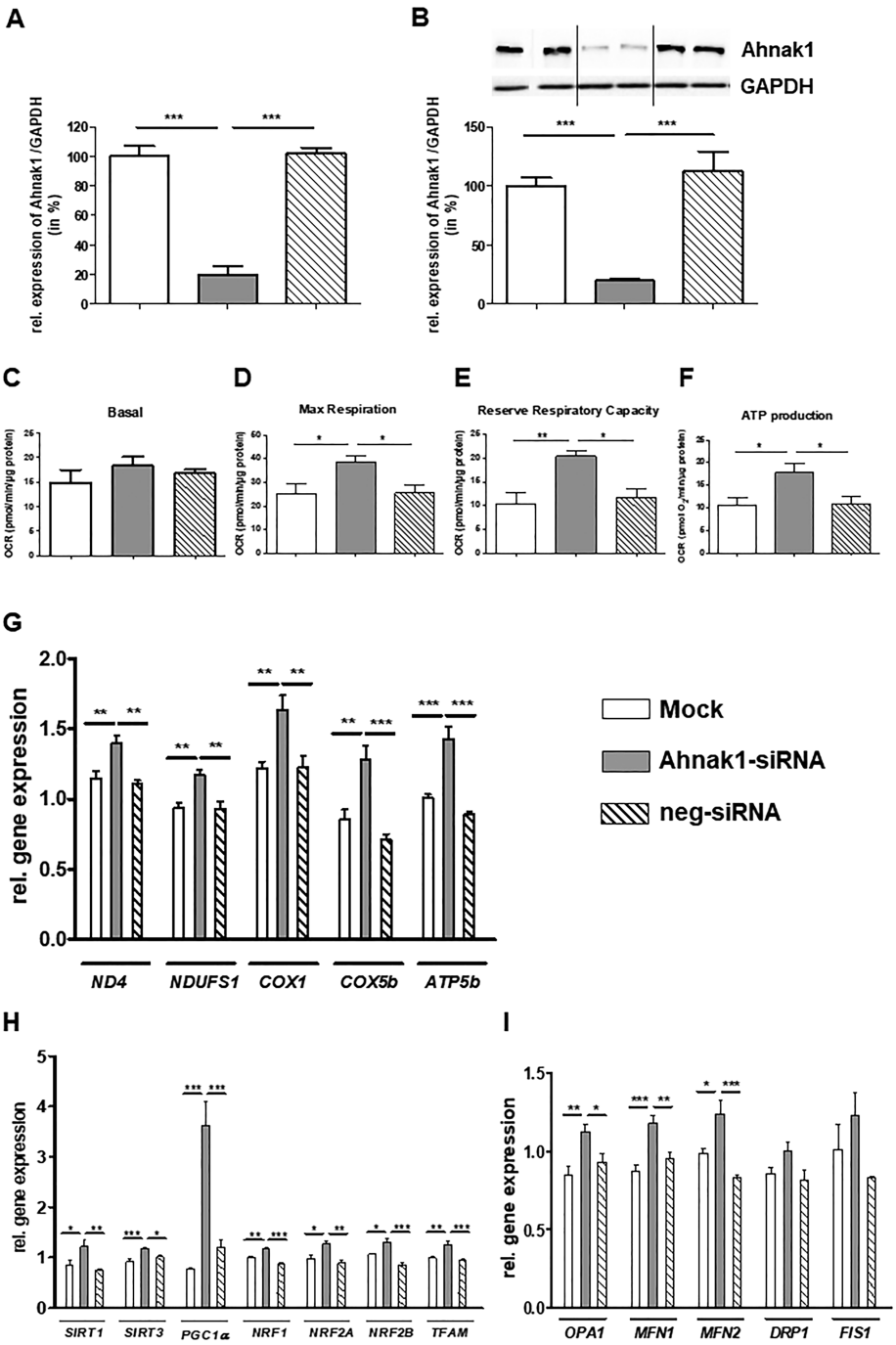

Figure 6 Attenuated Ahnak1 expression in AC16 cells improves mitochondrial function. AC16 cells were transiently transfected with Ahnak1-siRNA or neg-siRNA, or mock-transfected. Following experiments were conducted: after 72 h incubation, Ahnak1 mRNA und protein levels were determined by (A) reverse transcription polymerase chain reaction (RT-PCR) and (B) western blot analyses, respectively. The amount of Ahnak1 mRNA and protein of mock-transfected cells was set to 100% each. RT-PCR: n = 6–7 and western blot: n = 7 independent experiments in duplicates. (C–F) After 48 h incubation, parameters of respiratory control were measured. (C) Basal respiration; (D) maximal respiration; (E) spare respiratory capacity; (F) ATP production. Data were normalized by total protein content. OCR, oxygen consumption rate. n = 7 independent experiments per group, mean of 10 wells each. Data are represented as mean ± SEM. $^{*}P < 0.05$, $^{**}P < 0.01$, and $^{***}P < 0.001$, one-way analysis of variance followed by Bonferroni *post hoc* test. (G–I) The expression levels of mitochondrial genes (G), major regulators of mitochondrial gene expression (H), and main regulators of mitochondrial dynamics (I) were measured by RT-PCR in cells. Expression of target genes was normalized to the geometric mean of HPRT and GAPDH. Results are expressed as mean ± SEM of six to seven independent experiments in duplicates. $^{*}P < 0.05$, $^{**}P < 0.01$, $^{***}P < 0.001$, one-way analysis of variance followed by Bonferroni *post hoc* test.

(Ahnak1-siRNA), or non-targeting siRNA (neg-siRNA), or mock-transfected. Evaluation of knockdown efficiency showed that in cells transfected with Ahnak1-siRNA, the inhibition rates of Ahnak1 mRNA and protein expression were about 80% (*Figure* 6A and 6B). Transfection with neg-siRNA did not alter Ahnak1 expression levels, and these were comparable with those of mock-transfected cells, indicating that the inhibitory effect of Ahnak1-siRNA was specific.

To corroborate the involvement of Ahnak1 in the regulation of mitochondrial activity, we investigated whether the down-regulation of Ahnak1 would also affect the mitochondrial oxidative capacity in AC16 cells. Consistent with the data obtained from Ahnak1-KO cardiomyocytes, we observed a significant increase in mitochondrial activity in cells transfected with Ahnak1-siRNA, when compared with cells transfected with neg-siRNA or mock-transfected cells, as shown by significantly increased maximal respiration, respiratory reserve capacity, and ATP production (*Figure* 6C–6F). This indicates that cells with reduced Ahnak1 expression may be able to manage better an energetic crisis.

Following validation of the direct role of Ahnak1 in regulation of mitochondrial activity upon transfection with specific Ahnak1-targeted siRNA, we tested the effects of such treatment on the regulation of the expression of mitochondrial genes associated with OXPHOS complexes. Our data demonstrated that specific reduction of Ahnak1 expression led to increased expression of several nuclear and mitochondrial encoded genes such as *ND4* (NADH-dehydrogenase subunit 4), *NDUFS1* (NADH-dehydrogenase Fe–S subunit 1), *COX1* (cytochrome c oxidase subunit 1), *COX5b* (cytochrome c oxidase subunit 5B), and *ATP5b* (ATP synthase F1 subunit beta) (*Figure* 6G). Additionally, the specific Ahnak1 knockdown led also to significant increased expression of other transcription factors known to participate in the regulation of mitochondrial gene expression [e.g. *SIRT1* (NAD-dependent protein deacetylase sirtuin-1), *SIRT3* (NAD-dependent protein deacetylase sirtuin-3), *PGC1α* (peroxisome proliferator-activated receptor gamma coactivator 1-alpha), *NRF1* (nuclear respiratory factor 1), *NRF2A/2B*, (nuclear respiratory factor 2A and 2B), and *TFAM* (Transcription Factor A; *Figure* 6H)].

Furthermore, to assess the effects of Ahnak1 suppression on mitochondrial dynamic processes, the expression of genes involved in mitochondrial fusion and fission was compared between cells transfected with specific Ahnak1-siRNA and those of controls. Our data indicate that the specific

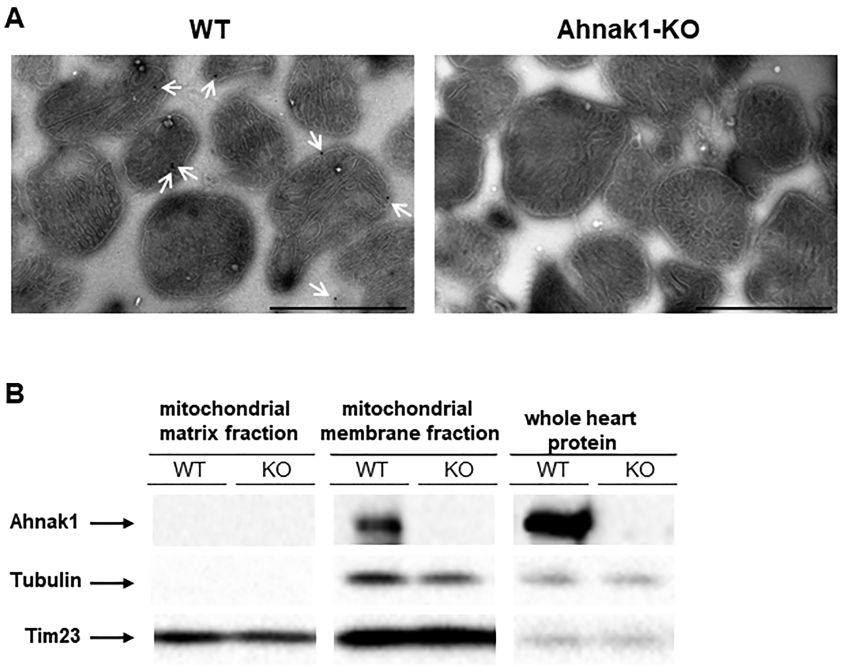

Figure 7 Ahnak1 is localized on mitochondrial membrane. (A) Immunoelectron microscopy for Ahnak1. Ultrathin sections prepared from isolated mitochondria from LV sections of aged adult Ahnak1-KO and their WT littermates were labelled with an anti-Ahnak1 mouse monoclonal antibody (E-5, Santa Cruz) and a 12 nm gold particle-conjugated secondary antibody. The gold particles were visualized by transmission electron microscopy. Ahnak1 staining was found mainly at the membrane of mitochondria isolated from the LV of WT mice (left panel) as indicated by arrows, whereas the mitochondria isolated from LV of Ahnak1-KO mice showed no signal (right panel). 16 000× magnification, scale bar: 1 μm. (B) Mitochondria isolated from freshly excised hearts of aged adult Ahnak1-KO and their age-matched WT littermates (n = 3–4 hearts per group) were evaluated by subcellular fractionation. The mitochondria were subfractionated in mitochondrial matrix and mitochondrial membrane fractions which were subjected to SDS-PAGE and western blotting. Ahnak1 was detected using an Ahnak1 antibody (Ahnak1-C1). Antibodies directed against Tim23 and tubulin were used as mitochondrial membrane and cytosolic marker, respectively. Whole proteins from hearts of Ahnak1-KO and WT mice were used as control. WT, wild type.

knockdown of Ahnak1 led to a significant increased expression of mitochondrial fusion markers, namely, *OPA1*, *MFN1*, and *MFN2* (*Figure* 6I). However, no significant differences in the expression of mitochondrial fission markers, *DRP1* and *FIS1*, were observed (*Figure* 6I). These data clearly indicate that Ahnak1 down-regulation is associated with the improvement of mitochondrial function in cardiomyocytes.

Ahnak1 is localized on mitochondrial membrane

On basis of our data, we assumed that Ahnak1 might be a key component of signalling involved in mitochondrial remodelling, because its down-regulation leads to attenuation of mitochondrial fragmentation. We therefore hypothesized that Ahnak1 might directly contact the mitochondrial surface. Indeed, our immunoelectron microscopy data with isolated mitochondrial fraction from aged adult WT hearts revealed that the Ahnak1 protein is mostly localized on the mitochondrial membrane (*Figure* 7A, left, arrows), whereas this signal was lacking on the mitochondria isolated from aged adult Ahnak1-KO hearts (*Figure* 7A, right). Consistently, analysis of isolated mitochondrial matrix and mitochondrial membrane fractions from heart tissues of aged adult Ahnak1-KO and WT littermates confirmed the presence of Ahnak1 in the mitochondrial membrane fraction of WT hearts (*Figur*e 7B). However, the signal for Ahnak1 was lacking in the mitochondrial matrix fraction of WT hearts, indicating that Ahnak1 is indeed localized only on the mitochondrial membrane. As expected, an anti-Ahnak1 antibody did not recognize a signal either in the mitochondrial membrane or in the mitochondrial matrix fractions prepared from Ahnak1-KO hearts (*Figure* 7B). Taken together, we could show that the Ahnak1 protein is localized on the mitochondrial membrane in the murine heart.

Discussion

A decline in mitochondrial function plays a key role in the aging process. Interventions that improve mitochondrial function are clinically significant in decelerating age-associated pathophysiological changes. In this study, using Ahnak1-KO mice, we demonstrated the crucial role of Ahnak1 on alterations of mitochondrial morphology and function in aged adult murine heart and TA muscle, and consequently, its influence on physical fitness in advanced age. *In vitro* studies using specific Ahnak1 targeted-siRNA in AC16 cells showed that the alteration of mitochondrial function is indeed a direct effect of Ahnak1. Finally, we presented Ahnak1 as a novel mitochondrial membrane-associated protein. Taken together, the data presented in this study indicate that the suppression of Ahnak1 may improve overall physical fitness and prevent adverse health outcomes with advancing age.

Although previous analyses of age-related changes in gene expression profiles reported that the expression of Ahnak1 is increased with age in skeletal muscles, and age-related increased expression of Ahnak1 gene inversely correlates with oxygen consumption and skeletal muscle fitness,[12,13,15] there was no conclusive explanation for the relationship between these phenomena so far. In this study, we showed that the level of Ahnak1 protein is also up-regulated with age in the murine heart and TA tissues and that the increased expression of Ahnak1 in aged adult mice exposed to treadmill running was associated with poor exercise tolerance, as most aged adult WT mice were unable to complete the running programme. By contrast, aged adult Ahnak1-KO mice showed enhanced running performance and a superior physical fitness. This discrepancy in running performance is indicative of compensation mechanisms in aged adult Ahnak1-KO mice that trigger an adaptive response to increased workload. Mitochondrial dysfunction is acknowledged as one of the hallmarks of aging, which leads to a decline in cellular function, and muscle frailty.[8,33] One of the potential mechanisms by which the suppression of Ahnak1 could increase the running capacity in aged adult mice is the improvement of mitochondrial function, thereby the mitochondria of Ahnak1-KO mice, as the primary source of ATP, can produce sufficient amounts of ATP to maintain the cardiac and skeletal muscle function.

Aging causes changes in the morphology of mitochondria in heart and skeletal muscle. Morphologically, the mitochondria of aged hearts appear to be more fragmented and circular in both human and animal models,[34,35] whereas aged skeletal muscles show either fragmented, rounded mitochondrial networks or enlarged mitochondria, depending on the muscle type or methodologies used.[26,36] In the present study, LV and TA tissues from both sexes of aged adult Ahnak1-KO mice showed that the number of enlarged/elongated mitochondria in these tissues was significantly increased, whereas the number of small mitochondria was significantly decreased in comparison with those of age-matched WT counterparts. The morphology of mitochondria is mainly regulated by fission and fusion processes, which are triggered by multiple proteins belonging to the family of large GTPases. MFN1 and MFN2 are required for the fusion of outer mitochondrial membranes, and OPA1 for the fusion of inner mitochondrial membranes, while the mitochondrial fission process is mainly mediated by the DRP1 and FIS1 proteins.[37] In this study, there were no significant differences in the expression of fission and fusion marker genes in the hearts between aged adult Ahnak1-KO and WT mice. This result, however, was not unexpected because the mitochondria in the heart are relatively immobile and have an extremely slow fusion and fission rate, so that the expression of these genes in the heart is very weak.[30,38] In contrast to the heart, however, we observed that the suppression/down-regulation of Ahnak1 in both aged adult TA muscles and in AC16 cells resulted in increased expression of the fusion markers

OPA1, *MFN1*, and *MFN2*, while the expression of the fission markers *FIS1* and *DRP1* remained unchanged. These data suggest that a shift in the mitochondrial fission-fusion balance towards fusion contributes to the observed changes in mitochondrial morphology from a fragmented state to a more enlarged/elongated state in cardiomyocytes and TA muscle of aged adult Ahnak1-KO mice.

Both experimental and mathematical models have demonstrated that elongated and enlarged mitochondria induced by fusion tend to have improved mitochondrial function (e.g. facilitating complementation of the mitochondrial genome, efficient metabolite exchange, increased respiration and ATP production, decreased reactive oxygen species production and reduced susceptibility to calcium overload).[39–41] In contrast, small/fragmented mitochondria induced by the fission process are more prone to mitophagy[42,43] and exhibit various functional disorders (e.g. decreased respiration and decreased ATP production).[41,44] The presence of more enlarged/elongated mitochondria in the LV and TA muscles of aged adult Ahnak1-KO mice may reflect that mitochondria in these muscles are more efficient and consequently produce more energy.

It has been shown that cardiac mitochondrial oxygen consumption decreases significantly with increasing age.[45] Interestingly, we observed that the mitochondria in aged adult Ahnak1-KO cardiomyocytes are able to overcome the decrease in oxygen consumption, as demonstrated by significantly increased mitochondrial maximal respiratory and maximal reserve respiratory capacity compared with those of aged adult WT cardiomyocytes. The direct effect of Ahnak1 on mitochondrial oxidative capacity was substantiated in AC16 cells. The attenuated Ahnak1 expression resulted in a significant increase in maximal respiration and maximal reverse respiratory capacity. The term 'reserve respiratory capacity' describes the amount of extra ATP that can be produced by oxidative phosphorylation in response to increased energy demand,[46] and its reduction contributes to a severe impairment of heart function and ultimately leads to the death of cardiac cells.[47]

Accordingly, ATP production requires proper functioning of the mitochondrial OXPHOS system which is composed of four electron transport chain complexes, namely, complexes I, II, III, and IV (cI, cII, cIII, and cIV), and the ATP synthase (cV), located within the mitochondrial inner membrane.[48] It has been demonstrated that the age-related reduction of oxygen consumption is a consequence of reduced functional activity of the OXPHOS system.[45,49] Previous human and animal studies on gene and protein expression revealed significant down-regulation of mitochondrial respiratory chain complexes in aging skeletal muscle and heart, particularly in interfibrillar mitochondria.[12,14,27,45,50] Interestingly, we observed in our study that suppression of the Ahnak1 gene in aged adult heart and TA muscles results in up-regulation of complexes cIII and cV expression compared with aged adult WT mice. There is some evidence that cIII plays a key role in maintaining the stability of the OXPHOS complexes in the mitochondria and protects them from degradation.[51] cV is important for the generation of energy in the form of ATP and its deficiency can cause a variety of diseases, including cardiomyopathy and skeletal muscle dysfunction.[52] Elevated cIII and cV levels in the heart and skeletal muscles of aged adult Ahnak1-KO mice could therefore be an attempt to improve the stability and function of the mitochondria and to restore the OXPHOS mechanisms, thus reversing the age-related decrease in ATP production in the mitochondria of both muscles.

Mitochondria have their own DNA, which encodes only 13 subunits of the OXPHOS system, but the remaining OXPHOX subunits and other mitochondrial proteins are encoded by the nucleus.[53] Therefore, coordinated communication between these two genomes is essential, which is largely controlled by a tightly orchestrated interaction of different transcriptional and metabolic regulators such as SIRT1, SIRT3, PGC1α, NRF1, NRF2, and TFAM.[54,55] Several studies demonstrated that changes in the expression and activity of these regulatory factors with age contribute to the loss of mitochondrial biogenesis and function.[56] In this study, we showed in AC16 cells, that the acute down-regulation of Ahnak1 the levels of representative mRNAs transcribed in the two genomes, such as *COX5b*, *COX1*, *NDUFS1*, *ND4*, and *ATP5b*, significantly increased. Additionally, the expression of *PGC1α*, *NRF1*, *NRF2A/B*, *TFAM*, *SIRT1*, and *SIRT3* genes, as crucial factors controlling the mitochondrial biogenesis, were also significantly increased in AC16 cells due to attenuated Ahnak1 expression. Therefore, our findings suggest that the increased expression of genes involved in the mitochondrial biogenesis is indeed a direct effect of attenuated Ahnak1 expression and not a secondary consequence of its systemic effects. The underlying molecular mechanisms have not yet been investigated in this study and should be addressed by future studies.

Cardiac and skeletal muscles, as tissues with high ATP turnover, require a constant ATP supply, mainly generated by mitochondrial oxidative phosphorylation, to sustain proper contractile function. However, the age-related reduced capacity of mitochondrial respiration and oxidative phosphorylation, as well as reduced mitochondrial biogenesis, compromise the ATP synthesis rates required for proper muscle contraction, resulting in faster muscle fatigue by limiting the supply of ATP to myocytes.[57,58] As expected, in line with the increased capacity of mitochondrial respiration and the more efficient oxidative phosphorylation in cardiac and TA muscles of aged adult Ahnak1-KO mice, we observed an improved cardiomyocyte contractile function and an increased fatigue resistance in TA muscles of aged adult Ahnak1-KO mice compared with the age-matched WT mice. Because the age-related decrease in contractile function is one of the main characteristics of frailty in older people, which is associated with poorer performance in daily activities and lower quality of life,[59,60] suppression of Ahnak1 expression

seems to be a promising alternative to improve muscular performance and thus the quality of life of older individuals.

Because Ahnak1 is mainly localized to the inner aspect of the plasma membrane (sarcolemma) of striated muscles,[10] it is therefore conceivable that Ahnak1 is also associated with the outer membrane of mitochondria. This assumption is supported by the fact that Ahnak1 is an interaction partner of myosin XIX (MYO19) that is associated with the mitochondrial outer membrane.[61–63] Our results showed that Ahnak1 is localized on the mitochondrial membrane, most likely at the outer mitochondrial membrane, and thus serves as a novel mitochondrial-associated-membrane protein. Based on the data obtained in this study, we assume that Ahnak1 binds to the contact sites on the mitochondrial membrane required for mitochondrial fusion, possibly masking these sites, which could disturb the mitochondrial fusion process. This is supported by the fact that the absence of Ahnak1 led to an increased mitochondrial fusion and thus to enlarged/elongated mitochondria in both cardiac and skeletal muscle tissues.

Conclusions

Exercise as a primary intervention can partially reverse age-related mitochondrial dysfunction. As demonstrated in this study, suppression of Ahnak1 can also lead to improved performance of aging cardiac and skeletal muscles. This finding could be of considerable importance for the elderly, who, for various reasons, are unable to be physically active or do exercise. For decades, studies have concentrated on drug-based approaches to restore mitochondrial function in age-related diseases, which have not yet been approved for release due to accompanying side effects. Because Ahnak1-deficient mice are viable and fertile into adulthood and show no cross-abnormalities,[10] and because we have shown that suppression of Ahnak1 even improves mitochondrial function in aging hearts and skeletal muscles, we believe that down-regulation of Ahnak1 could have preventive and therapeutic benefits for elderly individuals and improve their quality of life. Importantly, many studies showed that age-related cardiac, skeletal muscle, and mitochondrial disorder is a progressive process that begins already in middle age (long before there is any clear physical impact in the advanced old age), and a crucial point is to know the timing of age-related changes so that interventions to prevent them can be initiated before they occur. Taken together, our findings may have a significant impact not only on the understanding of the mechanisms of age-related mitochondrial dysfunction of cardiac and skeletal muscle but also suggests an intervention that may increase health span in the elderly.

Acknowledgements

We thank Petra Domaing, Karin Karczewski, Steffen Lutter, and Christina Schiel for excellent technical support. We also thank Dr Mercy M. Davidson from Columbia University for providing us with the AC16 cells. The authors of this manuscript certify that they comply with the ethical guidelines for authorship and publishing in the *Journal of Cachexia, Sarcopenia and Muscle*.[64]

Funding

The author(s) received no specific funding for this work.

Online supplementary material

Additional supporting information may be found online in the Supporting Information section at the end of the article.

Data S1. Supporting Information.
Table S1. Primers used for quantitative Real-Time Polymerase Chain Reaction.
Table S2. All antibodies used in immunoblot analysis.
Figure S1. (A) TD-NMRI analysis revealed that there are no significant differences in body weight, fat and muscle mass between aged adult Ahnak1-KO and WT littermates of both sexes at basal level (n = 10–11 mice/group). (B) Heart (left panels) and TA muscles (right panels) of aged adult Ahnak1-KO and WT mice of both sexes were isolated, weighed and correlated to body mass. Heart and TA masses were similar among all groups (n = 10–11 mice/group).
Figure S2. Expression of mitochondrial fusion and fission markers in the LV of aged adult male and female Ahnak1-KO and WT mice. (A-E) Real-time quantitative PCR was used to determine expression levels of fusion and fission markers *Opa1* (A), *Mfn1* (B), *Mfn2* (C), *Drp1* (D) and *Fis1* (E), respectively, in the LV tissues of aged adult WT and Ahnak1-KO mice. mRNA content of target genes was normalized to the geometric mean of *Hprt* and *Gapdh*. All data are expressed as means ± SEM, two-way ANOVA followed by Bonferroni post hoc test. (n = 7–8 hearts/group).

Conflict of interests

All authors declare that they have no conflict of interest.

References

1. United Nations DoEaSA, Population Division. World Population Ageing 2019 (ST/ESA/SER.A/444). 2020.
2. Franceschi C, Garagnani P, Morsiani C, Conte M, Santoro A, Grignolio A, et al. The continuum of aging and age-related diseases: common mechanisms but different rates. *Front Med (Lausanne)* 2018;**5**:61.
3. Fajemiroye JO, da Cunha LC, Saavedra-Rodriguez R, Rodrigues KL, Naves LM, Mourao AA, et al. Aging-induced biological changes and cardiovascular diseases. *Biomed Res Int* 2018;**2018**:7156435.
4. Bekfani T, Pellicori P, Morris DA, Ebner N, Valentova M, Steinbeck L, et al. Sarcopenia in patients with heart failure with preserved ejection fraction: impact on muscle strength, exercise capacity and quality of life. *Int J Cardiol* 2016;**222**:41–46.
5. Fulster S, Tacke M, Sandek A, Ebner N, Tschope C, Doehner W, et al. Muscle wasting in patients with chronic heart failure: results from the studies investigating co-morbidities aggravating heart failure (SICA-HF). *Eur Heart J* 2013;**34**:512–519.
6. Cruz-Jentoft AJ, Baeyens JP, Bauer JM, Boirie Y, Cederholm T, Landi F, et al. Sarcopenia: European consensus on definition and diagnosis: report of the European Working Group on Sarcopenia in Older People. *Age Ageing* 2010;**39**:412–423.
7. Sparling PB, Howard BJ, Dunstan DW, Owen N. Recommendations for physical activity in older adults. *BMJ* 2015;**350**:h100.
8. Boengler K, Kosiol M, Mayr M, Schulz R, Rohrbach S. Mitochondria and ageing: role in heart, skeletal muscle and adipose tissue. *J Cachexia Sarcopenia Muscle* 2017;**8**:349–369.
9. Tocchi A, Quarles EK, Basisty N, Gitari L, Rabinovitch PS. Mitochondrial dysfunction in cardiac aging. *Biochim Biophys Acta* 1847;**2015**:1424–1433.
10. Komuro A, Masuda Y, Kobayashi K, Babbitt R, Gunel M, Flavell RA, et al. The AHNAKs are a class of giant propeller-like proteins that associate with calcium channel proteins of cardiomyocytes and other cells. *Proc Natl Acad Sci U S A* 2004;**101**:4053–4058.
11. Davis TA, Loos B, Engelbrecht AM. AHNAK: the giant jack of all trades. *Cell Signal* 2014;**26**:2683–2693.
12. de Magalhaes JP, Curado J, Church GM. Meta-analysis of age-related gene expression profiles identifies common signatures of aging. *Bioinformatics* 2009;**25**:875–881.
13. Parida BP, Misra BB, Misra AN. Visual gene network analysis of aging-specific gene co-expression in human indicates overlaps with immuno-pathological regulations. *4open* 2018;**1**:15.
14. Su J, Ekman C, Oskolkov N, Lahti L, Strom K, Brazma A, et al. A novel atlas of gene expression in human skeletal muscle reveals molecular changes associated with aging. *Skelet Muscle* 2015;**5**:35.
15. Parikh H, Nilsson E, Ling C, Poulsen P, Almgren P, Nittby H, et al. Molecular correlates for maximal oxygen uptake and type 1 fibers. *Am J Physiol Endocrinol Metab* 2008;**294**:E1152–E1159.
16. Petzhold D, Lossie J, Keller S, Werner S, Haase H, Morano I. Human essential myosin light chain isoforms revealed distinct myosin binding, sarcomeric sorting, and inotropic activity. *Cardiovasc Res* 2011;**90**:513–520.
17. Davidson MM, Nesti C, Palenzuela L, Walker WF, Hernandez E, Protas L, et al. Novel cell lines derived from adult human ventricular cardiomyocytes. *J Mol Cell Cardiol* 2005;**39**:133–147.
18. Duft K, Schanz M, Pham H, Abdelwahab A, Schriever C, Kararigas G, et al. 17beta-Estradiol-induced interaction of estrogen receptor alpha and human atrial essential myosin light chain modulates cardiac contractile function. *Basic Res Cardiol* 2017;**112**:1.
19. Mahmoodzadeh S, Pham TH, Kuehne A, Fielitz B, Dworatzek E, Kararigas G, et al. 17beta-Estradiol-induced interaction of ERalpha with NPPA regulates gene expression in cardiomyocytes. *Cardiovasc Res* 2012;**96**:411–421.
20. Haase H, Pagel I, Khalina Y, Zacharzowsky U, Person V, Lutsch G, et al. The carboxyl-terminal ahnak domain induces actin bundling and stabilizes muscle contraction. *FASEB J* 2004;**18**:839–841.
21. Mahmoodzadeh S, Fritschka S, Dworatzek E, Pham TH, Becher E, Kuehne A, et al. Nuclear factor-kappaB regulates estrogen receptor-alpha transcription in the human heart. *J Biol Chem* 2009;**284**:24705–24714.
22. Slot JW, Geuze HJ. Cryosectioning and immunolabeling. *Nat Protoc* 2007;**2**:2480–2491.
23. Kargel E, Menzel R, Honeck H, Vogel F, Bohmer A, Schunck WH. Candida maltosa NADPH-cytochrome P450 reductase: cloning of a full-length cDNA, heterologous expression in *Saccharomyces cerevisiae* and function of the N-terminal region for membrane anchoring and proliferation of the endoplasmic reticulum. *Yeast* 1996;**12**:333–348.
24. Chen Q, Samidurai A, Thompson J, Hu Y, Das A, Willard B, et al. Endoplasmic reticulum stress-mediated mitochondrial dysfunction in aged hearts. *Biochim Biophys Acta Mol Basis Dis* 1866;**2020**:165899.
25. Judge S, Jang YM, Smith A, Hagen T, Leeuwenburgh C. Age-associated increases in oxidative stress and antioxidant enzyme activities in cardiac interfibrillar mitochondria: implications for the mitochondrial theory of aging. *FASEB J* 2005;**19**:419–421.
26. Leduc-Gaudet JP, Picard M, St-Jean Pelletier F, Sgarioto N, Auger MJ, Vallee J, et al. Mitochondrial morphology is altered in atrophied skeletal muscle of aged mice. *Oncotarget* 2015;**6**:17923–17937.
27. Lesnefsky EJ, Gudz TI, Moghaddas S, Migita CT, Ikeda-Saito M, Turkaly PJ, et al. Aging decreases electron transport complex III activity in heart interfibrillar mitochondria by alteration of the cytochrome c binding site. *J Mol Cell Cardiol* 2001;**33**:37–47.
28. Tirone M, Tran NL, Ceriotti C, Gorzanelli A, Canepari M, Bottinelli R, et al. High mobility group box 1 orchestrates tissue regeneration via CXCR4. *J Exp Med* 2018;**215**:303–318.
29. Sohal RS, Bridges RG. Associated changes in the size and number of mitochondria present in the midgut of the larvae of the housefly, *Musca domestica* and phospholipid composition of the larvae. *J Cell Sci* 1978;**34**:65–79.
30. Dorn GW 2nd. Mitochondrial dynamism and heart disease: changing shape and shaping change. *EMBO Mol Med* 2015;**7**:865–877.
31. Dorn G II. Mitochondrial fission/fusion and cardiomyopathy. *Curr Opin Genet Dev* 2016;**38**:38–44.
32. Crupi AN, Nunnelee JS, Taylor DJ, Thomas A, Vit JP, Riera CE, et al. Oxidative muscles have better mitochondrial homeostasis than glycolytic muscles throughout life and maintain mitochondrial function during aging. *Aging (Albany NY)* 2018;**10**:3327–3352.
33. Figueiredo PA, Mota MP, Appell HJ, Duarte JA. The role of mitochondria in aging of skeletal muscle. *Biogerontology* 2008;**9**:67–84.
34. Cheng Z, Ito S, Nishio N, Thanasegaran S, Fang H, Isobe K. Characteristics of cardiac aging in C57BL/6 mice. *Exp Gerontol* 2013;**48**:341–348.
35. El'darov Ch M, Vays VB, Vangeli IM, Kolosova NG, Bakeeva LE. Morphometric examination of mitochondrial ultrastructure in aging cardiomyocytes. *Biochemistry (Mosc)* 2015;**80**:604–609.
36. Halling JF, Ringholm S, Olesen J, Prats C, Pilegaard H. Exercise training protects against aging-induced mitochondrial fragmentation in mouse skeletal muscle in a PGC-1alpha dependent manner. *Exp Gerontol* 2017;**96**:1–6.
37. Liesa M, Palacin M, Zorzano A. Mitochondrial dynamics in mammalian health and disease. *Physiol Rev* 2009;**89**:799–845.
38. Song M, Dorn GW 2nd. Mitoconfusion: noncanonical functioning of dynamism factors in static mitochondria of the heart. *Cell Metab* 2015;**21**:195–205.
39. Chen Y, Liu Y, Dorn GW 2nd. Mitochondrial fusion is essential for organelle function and cardiac homeostasis. *Circ Res* 2011;**109**:1327–1331.
40. Hoitzing H, Johnston IG, Jones NS. What is the function of mitochondrial networks? A theoretical assessment of hypotheses

and proposal for future research. *Bioessays* 2015;**37**:687–700.
41. Ong SB, Subrayan S, Lim SY, Yellon DM, Davidson SM, Hausenloy DJ. Inhibiting mitochondrial fission protects the heart against ischemia/reperfusion injury. *Circulation* 2010;**121**:2012–2022.
42. Gomes LC, Scorrano L. Mitochondrial morphology in mitophagy and macroautophagy. *Biochim Biophys Acta* 1833;**2013**:205–212.
43. Romanello V, Guadagnin E, Gomes L, Roder I, Sandri C, Petersen Y, et al. Mitochondrial fission and remodelling contributes to muscle atrophy. *EMBO J* 2010;**29**: 1774–1785.
44. Jheng HF, Tsai PJ, Guo SM, Kuo LH, Chang CS, Su IJ, et al. Mitochondrial fission contributes to mitochondrial dysfunction and insulin resistance in skeletal muscle. *Mol Cell Biol* 2012;**32**:309–319.
45. No MH, Heo JW, Yoo SZ, Kim CJ, Park DH, Kang JH, et al. Effects of aging and exercise training on mitochondrial function and apoptosis in the rat heart. *Pflugers Arch* 2020;**472**:179–193.
46. Desler C, Hansen TL, Frederiksen JB, Marcker ML, Singh KK, Juel Rasmussen L. Is there a link between mitochondrial reserve respiratory capacity and aging? *J Aging Res* 2012;**2012**:192503.
47. Sansbury BE, Jones SP, Riggs DW, Darley-Usmar VM, Hill BG. Bioenergetic function in cardiovascular cells: the importance of the reserve capacity and its biological regulation. *Chem Biol Interact* 2011;**191**: 288–295.
48. Emelyanova L, Preston C, Gupta A, Viqar M, Negmadjanov U, Edwards S, et al. Effect of aging on mitochondrial energetics in the human atria. *J Gerontol A Biol Sci Med Sci* 2018;**73**:608–616.
49. Dai DF, Rabinovitch PS, Ungvari Z. Mitochondria and cardiovascular aging. *Circ Res* 2012;**110**:1109–1124.
50. Zahn JM, Sonu R, Vogel H, Crane E, Mazan-Mamczarz K, Rabkin R, et al. Transcriptional profiling of aging in human muscle reveals a common aging signature. *PLoS Genet* 2006;**2**:e115.
51. Protasoni M, Perez-Perez R, Lobo-Jarne T, Harbour ME, Ding S, Penas A, et al. Respiratory supercomplexes act as a platform for complex III-mediated maturation of human mitochondrial complexes I and IV. *EMBO J* 2020;**39**:e102817.
52. Braczynski AK, Vlaho S, Muller K, Wittig I, Blank AE, Tews DS, et al. ATP synthase deficiency due to TMEM70 mutation leads to ultrastructural mitochondrial degeneration and is amenable to treatment. *Biomed Res Int* 2015;**2015**:462592.
53. Garnier A, Fortin D, Zoll J, N'Guessan B, Mettauer B, Lampert E, et al. Coordinated changes in mitochondrial function and biogenesis in healthy and diseased human skeletal muscle. *FASEB J* 2005;**19**:43–52.
54. Popov LD. Mitochondrial biogenesis: an update. *J Cell Mol Med* 2020;**24**: 4892–4899.
55. Ventura-Clapier R, Garnier A, Veksler V. Transcriptional control of mitochondrial biogenesis: the central role of PGC-1alpha. *Cardiovasc Res* 2008;**79**:208–217.
56. Moreira OC, Estebanez B, Martinez-Florez S, de Paz JA, Cuevas MJ, Gonzalez-Gallego J. Mitochondrial function and mitophagy in the elderly: effects of exercise. *Oxid Med Cell Longev* 2017;**2017**:2012798.
57. Chabi B, Ljubicic V, Menzies KJ, Huang JH, Saleem A, Hood DA. Mitochondrial function and apoptotic susceptibility in aging skeletal muscle. *Aging Cell* 2008;**7**: 2–12.
58. Porter C, Hurren NM, Cotter MV, Bhattarai N, Reidy PT, Dillon EL, et al. Mitochondrial respiratory capacity and coupling control decline with age in human skeletal muscle. *Am J Physiol Endocrinol Metab* 2015;**309**: E224–E232.
59. Celis-Morales CA, Welsh P, Lyall DM, Steell L, Petermann F, Anderson J, et al. Associations of grip strength with cardiovascular, respiratory, and cancer outcomes and all cause mortality: prospective cohort study of half a million UK Biobank participants. *BMJ* 2018;**361**:k1651.
60. Mueller-Schotte S, Bleijenberg N, van der Schouw YT, Schuurmans MJ. Fatigue as a long-term risk factor for limitations in instrumental activities of daily living and/or mobility performance in older adults after 10 years. *Clin Interv Aging* 2016;**11**: 1579–1587.
61. Bocanegra JL, Fujita BM, Melton NR, Cowan JM, Schinski EL, Tamir TY, et al. The MyMOMA domain of MYO19 encodes for distinct Miro-dependent and Miro-independent mechanisms of interaction with mitochondrial membranes. *Cytoskeleton (Hoboken)* 2020;**77**:149–166.
62. Oeding SJ, Majstrowicz K, Hu XP, Schwarz V, Freitag A, Honnert U, et al. Identification of Miro1 and Miro2 as mitochondrial receptors for myosin XIX. *J Cell Sci* 2018;**131**:jcs219469.
63. Quintero OA, DiVito MM, Adikes RC, Kortan MB, Case LB, Lier AJ, et al. Human Myo19 is a novel myosin that associates with mitochondria. *Curr Biol* 2009;**19**: 2008–2013.
64. von Haehling S, Morley JE, Coats AJS, Anker SD. Ethical guidelines for publishing in the Journal of Cachexia, Sarcopenia and Muscle: update 2019. *J Cachexia Sarcopenia Muscle* 2019;**10**:1143–1145.